ミリ波帯における360度映像伝送に関する検討

Lu YuJun[1] 小林 真[1,†1] 藤橋 卓也[1] 猿渡 俊介[1] 渡辺 尚[1]

概要：With the explosive growth in mobile data demand, wireless multimedia technologies are developing towards providing an immersive experience for the users. 360-degree video delivery, i.e., omnidirectional video delivery, over wireless links is one of the new multimedia techniques to provide an omnidirectional view of three-dimensional scenes for wireless virtual reality applications. Since the resolution and frame rate of 360-degree video are even high, conventional schemes on 360-degree video delivery use digital-based video compression for traffic reduction. However, a large computation time in the digital-based video compression may degrade the quality of immersive experience because such immersive contents require an extremely low end-to-end latency between the content server and client to realize a good immersion. To realize high-quality and low-delay wireless 360-degree video delivery, this paper proposes a novel system of wireless 360-degree video delivery over millimeter wave (mmWave) networks. Specifically, the proposed system divides the uncompressed 360-degree video into multiple tiles and then assigns the tiles to multiple 60 GHz mmWave antennas placed around the Head Mounted Display (HMD) user based on the user's direction. Finally, each mmWave antenna sends the assigned tiles to the user based on the 60 GHz channel state information (CSI) and the user's watching tile. It is demonstrated that our system can provide a sufficient data rate even for 360-degree video with 8K resolution at 60 frames/second (fps) without video compression.

キーワード：360-degree video, 60 GHz mmWave, MIMO, HMD

1. Introduction

From the last century, Virtual Reality (VR) technology has been received extensive attention by developers, engineers, and researchers. For example, Oculus Rift, which is a VR HMD, had launched in 2012 and brought people's vision back into VR. Until now, there are many off-the-shelf wired and wireless HMDs, e.g., HTC Vive and PSVR in wired HMDs and Google cardboard 2 and Gear VR in wireless HMDs, for VR applications. VR can be applied to numerous application scenarios such as virtual shopping, chat, travel, education, and even mountain climbing.

360-degree video delivery is a key component to provide good immersion in such VR applications. In contrast to conventional videos, the 360-degree video contains a 360-degree view of the three-dimensional (3D) scene captured by an omnidirectional camera and the captured videos are mapped onto a two-dimensional (2D) plane using a certain projection, e.g., equirectangular projection. The sender transmits the mapped video to the HMD user via wireless links. The user can watch a part of the received 360-degree video, called viewport, through the HMD. In addition, each user freely moves the watching viewport during video playback, and thus the user can achieve a novel experience and truly feel the virtual world.

On the other hand, 360-degree video delivery over wireless links has a challenging issue. Specifically, the resolution requirement of the 360-degree video is even high such as 8K ($7,680 \times 4,320$) with 60 fps and more to reproduce 3D scenes on human eyes. In this case, bit rate more than 47 Gbps is required for uncompressed 360-degree video delivery.

To deliver 360-degree video over wireless links, one of the simplest methods on 360-degree video delivery is to encode the 360-degree video using digital-based video compression before transmission and decode the encoded 360-degree video before playback. However, encoding and decoding of 360-degree video may cause a large computing time, and thus it makes it inherently difficult to realize real-time immersive applications. Although the existing studies on 360-degree video delivery [1–11] consider the user's future viewport and selectively encode and transmit the viewport to HMD user, it still causes a large computing time for encoding and decoding. In addition, an erroneous prediction of user's future viewport causes a large re-transmission delay to receive the desired view-

[1] 大阪大学大学院情報科学研究科
[†1] 現在，広島市立大学大学院情報科学研究科

port. Other existing studies [1, 7] divide 360-degree video frames into multiple tiles, and then encode and stream all the tiles. In this case, the sender encodes the tiles out of the user's future viewport into low video quality. They reduce re-transmission delay because of the reduction on the impact of an erroneous prediction of user's viewport while such adaptive video coding may cause further long computing delay.

This paper proposes a new delivery system of wireless 360-degree video delivery to overcome the above-mentioned issues, motivated by mmWave communication and Multiple Input Multiple Output (MIMO) techniques. The proposed system uses four 60 GHz mmWave antennas deployed around the wireless HMD user. To deliver 360-degree video by using the 60 GHz mmWave antennas, the sender divides the uncompressed 360-degree video into four tiles and then assigns the divided tiles to four 60 GHz mmWave antennas based on the HMD user's direction. Finally, each 60 GHz mmWave antenna sends the assigned tile to the wireless HMD user based on the 60 GHz channel CSI and the user's watching viewport. The contributions of our work are as follows:

- A system of low-delay wireless 360-degree video delivery without video compression is designed by using multiple mmWave antennas via the frequency band of 60 GHz.
- An indoor mmWave channel model is used to analyze the performance of the proposed scheme in the multi-antenna and single-user scenario.
- A partial signal processing based on zero-forcing (ZF) precoding is used to discuss the impact of CSI for wireless 360-degree video delivery.

Evaluations show that our proposed system can sustainably yield sufficient data rate to send the uncompressed 360-degree video even with 8K resolution at 60 fps.

The remainder of this paper is organized as follows. Our proposed system is described in Section 2. Section 3 describes the system model of 60 GHz channel and video transmission. Section 4 presents the evaluation results. The related work and the conclusion are concluded in Section 5 and Section 6, respectively.

2. Proposed Approach

This paper proposes a viewport-dependent wireless 360-degree video delivery system using 60 GHz mmWave frequency band utilized in the IEEE 802.11ad standard to achieve stable multi-Gbps throughput.

Fig. 1 shows an overview of the proposed system. The server pre-sends the compressed video to the PC via content delivery networks, and then the PC obtains the reconstructed 360-degree video by decoding the received bitstream. The PC is connected to four mmWave antennas, which are set in four directions of the HMD user, via wires. According to the position information from the user's HMD, the reconstructed 360-degree videos are divided into four tiles and the PC assigns four tiles to four antennas. Each mmWave antenna transmits the assigned tile to the HMD user over 60 GHz channel under the same bandwidth. In this case, for avoiding the interference between different transmission antennas, each mmWave antenna uses ZF precoding to achieve a nearly optimal capacity. For ZF precoding, HMD sends CSI as feedback depending on the channel sounding interval.

This paper focuses on the transmission between four antennas and HMD in order to verify whether the proposed system can support the stable transmission rate for ultra-high resolution of 360-degree video. Fig. 2 illustrates the timing diagram of video transmission between the antennas and HMD user.

Firstly, the position information of user's HMD is transmitted to the PC. At the same time, Null Data Packet (NDP) is sent from transmission antennas to HMD to capture the current CSI. After PC received the position information, the PC uses the last 10 or more position samples for viewport prediction. Specifically, Weighted Linear Regression (WLR) is applied across the samples to predict the user's future viewport. The tile corresponding to the predicted viewport is assigned to all the transmission antennas. The tiles other than the predicted viewport are assigned to the other transmission antennas to avoid quality degradation due to sudden HMD movement. The PC transfers the divided tiles to the transmission antennas via wires. In addition, because the location of antennas and HMD is static, the PC predicts CSI to build a precoding matrix used for ZF precoding across the transmission antennas based on the difference between predicted user's direction and each transmission antenna. The transmission antenna corresponding to the predicted direction sends the assigned tiles to the HMD. After the PC received CSI feedback from user's HMD, the PC modifies the precoding matrix $\boldsymbol{W}$ based on the received CSI. In addition, they update the position information based on the relationship between the received CSI and user's HMD orientation to improve the accuracy of viewport estimation. Finally, they send the rest of the tiles to the HMD.

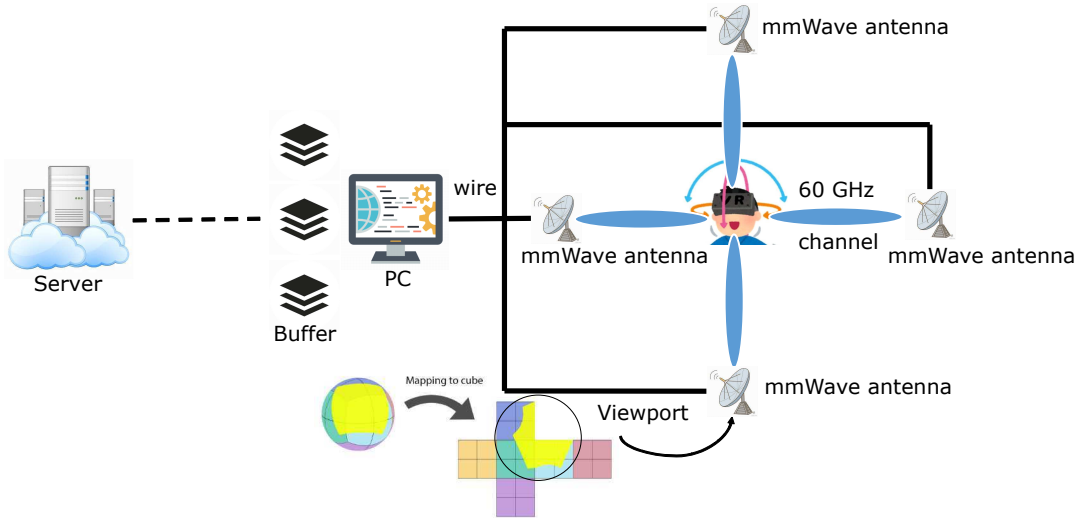

Fig. 1: A 60 GHz mmWave based wireless 360-degree video transmission system

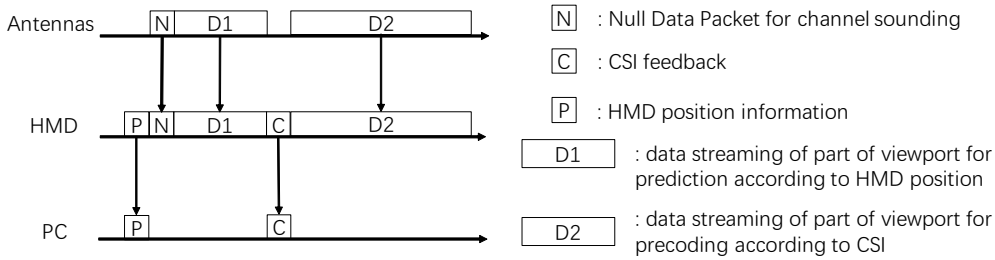

Fig. 2: Timing diagram of video transmission between antennas and HMD user

3. System Model

This section presents the mathematical models of wireless 60 GHz mmWave channel and spatial signal processing over MIMO system, and further formulates the performance of the uncompressed 360-degree video transmission in terms of Peak Signal to Noise Ratio (PSNR).

A. 60 GHz Channel Model

The received signal strength $P^{\mathrm{r}}_{\mathrm{dBm}}$ in 60 GHz mmWave channel is defined as follows:

$$P^{\mathrm{r}}_{\mathrm{dBm}} = P^{\mathrm{t}}_{\mathrm{dBm}} + G^{\mathrm{t}}_{\mathrm{dBi}} + L\left(d\right) + G^{\mathrm{r}}_{\mathrm{dBi}} \qquad (1)$$

where $P^{\mathrm{t}}_{\mathrm{dBm}}$, $G^{\mathrm{t}}_{\mathrm{dBi}}$, $G^{\mathrm{r}}_{\mathrm{dBi}}$, and $L\left(d\right)$ are the transmission power, the transmission antenna gain, the received atenna gain, and the path loss in dB, respectively.

We note that antenna patterns are complex and require many details to accurately describe the real antennas. For this reason, the proposed system assumes the transmission antennas and user's HMD are all equipped with a basic steerable antenna [12]. The main lobe gain is described using a circularly symmetric Gaussian function which is represented in analytical form as follows:

$$G\left(\theta,\phi\right) = \begin{cases} G_0 - 3.01 \times \left(\frac{2\theta}{\theta_{-3\mathrm{dB}}}\right)^2 & 0 \le \theta \le \theta_{\mathrm{ml}}/2 \\ -0.4111 \times \ln\left(\theta_{-3\mathrm{dB}}\right) - 10.597 & \theta_{\mathrm{ml}}/2 \le \theta \le 180^\circ \end{cases} \qquad (2)$$

where θ, ϕ, $\theta_{-3\mathrm{dB}}$, and θ_{ml} are the elevation angle, azimuth angle, half-power beam width (HPBW) angle, and main lobe beam angle, respectively. Specifically, θ_{ml} is defined as $\theta_{\mathrm{ml}} = 2.6 \times \theta_{-3\mathrm{dB}}$ and represents the boundary between the main lobe and the side lobe. G_0 is a maximum antenna gain when the elevation angle θ is 0 degree which can be calculated as follows:

$$G_0 = 10 \log \left[\frac{1.6162}{\sin\left(\theta_{-3\mathrm{dB}}/2\right)}\right]^2.$$

The above model is applicable provided when the HPBW angle $\theta_{-3\mathrm{dB}}$ is less than 80 degree. According to the different elevation angle θ, $G\left(\theta,\phi\right)$ can be used to compute $G^{\mathrm{t}}_{\mathrm{dBi}}$ and $G^{\mathrm{r}}_{\mathrm{dBi}}$ in (1).

Based on the IEEE 802.11ad channel model [13], the dB scaled 60 GHz line-of-sight (LOS) path loss $L\left(d\right)$ for the living room environment can be calculated as follows:

$$L\left(d\right) = \mathrm{A}_{\mathrm{LOS}} + 20\log_{10}\left(f\right) + 10 n_{\mathrm{LOS}} \log_{10}\left(d\right)$$

where $\mathrm{A}_{\mathrm{LOS}}$ has a specific value for the basic steerable directional antenna model, that is, $\mathrm{A}_{\mathrm{LOS}} = 32.5$, as defined

in [13]. The path loss coefficient n_{LOS} is set to 2 for the living room. In addition, f (GHz) is the carrier frequency, d (m) is the distance between transmission antenna and HMD.

After the calculation of the received signal strength without interference such as a single transmission antenna and multiple subchannels, the receiver sensitivity is used as background noise to compute signal-to-noise ratio (SNR):

$$\mathrm{SNR}_{\mathrm{dB}}^{\mathrm{NoI}} = P_{\mathrm{dBm}}^{\mathrm{r}} - n_{\mathrm{dB}} \tag{3}$$

where n_{dB} is a receiver sensitivity of modulation and coding scheme (MCS) level k which is defined in IEEE 802.11ad specification.

When considering interference from other signals of the same frequency band, the interference signal is added to the received signal. The signal-to-interference plus noise ratio (SINR) in a dB scale can be defined as follows:

$$\mathrm{SINR}_{\mathrm{dB}} = P_{\mathrm{dBm}}^{\mathrm{r}} - 10\log_{10}\left(n_{\mathrm{W}} + \sum_{i\in \mathrm{T_x}\setminus r} I_{\mathrm{W}}^{i}\right) \tag{4}$$

where $\sum_{i\in \mathrm{T_x}\setminus r} I_{\mathrm{W}}^{i}$ is the sum of the interference from another antenna i in the set of transmission antennas except the antenna r which is located against the user's HMD.

Since calculated SNR or SINR in (3) and (4), the theoretical channel capacity based on the Shannon–Hartley theorem can be formulated as follows:

$$C = B\log_2\left(1 + 10^{\frac{\mathrm{SNR_{dB}}}{10}}\right) \tag{5}$$

where B is channel bandwidth for 60 GHz wireless transmission system. This paper defines the bandwidth as 2.16 GHz.

B. Zero Forcing Precoding

Since considering 360-degree video delivery through a mmWave wireless channel with multiple transmission antennas, the proposed system assumes the PC receives CSI depending on channel sounder via channel feedback from HMD. In order to reduce the interference from other antennas, ZF precoding [14] is adopted to decouples the multi-user channel into multiple independent subchannels to solve the interference problem.

Considering M transmission antennas and N users with a single received antenna, the received signal is expressed as follows:

$$y_n = h_n^T x + z_n, \quad n = 1, 2, \ldots, N \tag{6}$$

where $h_n \in \mathbb{R}^{M\times 1}$ is the wireless channel vector for user n, z_n is an effective noise for the user n with zero mean and variance σ^2.

In addition, the distance $d_{i,j}$ between any two antennas i, j is satisfied with the condition of $d_{i,j} \gg \frac{\lambda}{2}$. In this case, the elements of the channel matrix h_n are randomly generated independent and identically distributed (i.i.d.) random variables generated by a random seed to follow the standard normal distribution.

For interference reduction, $\boldsymbol{W} \in \mathbb{R}^{1\times M}$ vector is designed to achieve zero interference between transmission antennas. By precoding in the transmission antennas, the signals sent by other antennas are orthogonal to the signals required by the receiving antenna, i.e., $[\boldsymbol{HW}]_{m,l} = 0$, if $m \neq l$. Then, for all the users, $\boldsymbol{HW}$ can be expressed as

$$\boldsymbol{HW} = \mathrm{diag}\{\sqrt{p}\}$$

where $\sqrt{p} = [\sqrt{p_1}\ \sqrt{p_2} \cdots \sqrt{p_M}]^T$.

$\boldsymbol{W}$ can be obtained via pseudo-inverse of the channel matrix [14], that is

$$\boldsymbol{W} = \boldsymbol{H}^T\left(\boldsymbol{H}\boldsymbol{H}^T\right)^{-1}\mathrm{diag}\{\sqrt{p}\} \tag{7}$$

With ZF precoding, the received signal in (6) can be realized as $y = x + n$ for each user. The SNR of the user n with ZF precoding is

$$\mathrm{SNR}_{\mathrm{dB}}^{\mathrm{ZF}} = P_{\mathrm{dBm}}^{\mathrm{r}} - n_{\mathrm{dB}} - \gamma_n, \tag{8}$$

and will be decreased by $\gamma_n = \left(\sum_{m=1}^{M} h_{nm}w_{mn}\right)^2$ compared to the ideal situation without interference ($\mathrm{SNR}_{\mathrm{dB}}^{\mathrm{NoI}}$). Therefore, during simulation verification, the channel state of each antenna is roughly estimated by calculating SNR.

C. Video Transmission Process

In order to realize high-quality 360-degree video delivery, this paper assumes the resolution and frame rate of the 360-degree video are 7680 × 4320 and 60 fps, and thus it requires more than 47 Gbps. The bitstream is divided into multiple data packets and each of them has 1500 bytes data, then the packets are sent from transmission antennas to HMD according to binary phase-shift keying (BPSK).

The energy per symbol to noise power spectral density $\frac{E_s}{N_0}$ ($E_b = E_s$ for BPSK modulation) can be derived from $\mathrm{SNR}_{\mathrm{dB}}$ in (3), (4), or (8) in different scenarios:

$$\mathrm{SNR}_{\mathrm{dB}} = 10\log_{10}\left(\frac{E_b \times f_b}{N_0 \times B}\right)$$

where E_b, f_b and N_0 are signal power for each symbol in

Table. 1: Simulation parameters

transmission antenna power	8.09 dBm
Noise sensitivity	−87 dBm
Bandwidth	2.16 GHz
Bit rate	47.78 Gbps
Distance	3 m
Path loss	−77.55 dBm
Packet size	1500 byte

Table. 2: Required bit-rate in each resolution of video

video	resolution	bit rate
8K	7680 × 4320	47.78 Gbps
4K	3840 × 2160	11.94 Gbps
2K	2048 × 2050	6.05 Gbps
1080P	1920 × 1080	2.99 Gbps

watts, bit rate in bits per second, and noise power.

We calculate the bit error rate (BER) during the above transmission process. In addition, this paper defines that a packet is incorrect even if one bit is erroneous. Thus, the packet error ratio (PER) can be formulated as follows:

$$\mathrm{PER} = 1 - (1 - \mathrm{BER})^{N}$$

where N is the number of bits in data packet. For small bit error probabilities and large data packets, PER is approximately $\mathrm{PER} = \mathrm{BER} \times N$.

After all, the following equation is used to compute the PSNR of the video:

$$\mathrm{PSNR} = \sum_{p \in \mathrm{N}_p} \left(\frac{\mathrm{PSNR}_p \times \mathrm{PER}_{p,\mathrm{dB}}}{\mathrm{N}_p} \right) \qquad (9)$$

where PSNR_p is the ideal PSNR related to encoding, decoding, and transmission process between the server and the PC. In addition, $\mathrm{PER}_{p,\mathrm{dB}}$, N_p are the PER of the corresponding packet and the number of packets for the whole transmitted 360-degree video.

4. Evaluation

This section evaluates the performance of the proposed system using MATLAB. The simulation parameters are defined in Table. 1. The proposed system considers a small rectangular area (6m × 6m) in the living room with four transmission antennas on the wall. Each antenna is connected with a PC via a wire. In addition, one user sits on the center of the living room. In this case, the distance between the user and each antenna is 3 meters. We assume the four transmission antennas and HMD are equipped with Qualcomm QCA6300 series chipset [15]. The MCS of the receiver is set to MCS0, and thus the receiver minimum sensitivity is set to -87 dBm. MCS0 uses BPSK modulation, 1/2 coding rate, and a single spatial stream. In addition, transmission power with antenna gain is set to 24 dBm. According to the transmission antenna gain in (2), the transmission power is 8.07 dBm at HPBW angle of 30 degree. Our system is evaluated against three schemes:

- oneTx: the user only receives video from one mmWave antenna. The antenna sends the entire frame using the entire 2.16 GHz bandwidth.
- subChannel: the user receives the tiles from four mmWave antennas over different subchannels. Here, the bandwidth of each subchannel is 0.54 GHz.
- sendDirect: the user receives the tiles from four mmWave antennas using the entire 2.16 GHz bandwidth without using ZF precoding.

A. Channel State

This section first evaluates the SNR performance of 60 GHz channel in each reference scheme as a function of the user's receiving angle of θ. For the sake of simulation, one 360-degree video frame is divided into four same-sized tiles and the PC assigns them to the four antennas. In this case, the bit rate of each antenna is one-quarter of the bit rate of the full 360-degree video. With the ZF precoding, the average noise enhancement for SNR is estimated by ten times Monte-Carlo simulations for each receiving angle θ.

In Fig. 3, we evaluate the SNR performance with different HPBW angles to discuss the effect of the antenna gain and the main lobe width of the 60 GHz mmWave antennas. We can see that SNR performance of the proposed system is approximately the same as the subChannel scheme which is assumed that there is no interference between subchannels. The maximum degradation of the SNR between the proposed system and subChannel scheme is about 5 dB. In Fig. 3 (a), because the HPBW is low, the oneTx scheme is better than our system for 67.78% of the user's receiving angle. If HPBW angle is set to more than 45 degrees, our proposed system outperforms oneTx scheme in the most of the receiving angles. Specifically, at HPBW angle of 80 degree, the proportion goes down to 31.67% in Fig. 3 (d). In addition, sendDirect scheme leads to the worst channel state in any case.

B. Maximum Supported Video

Then the channel capacity of each reference scheme is evaluated according to (5). Based on the channel capacity and the required bit rate in Table. 2, the supported video

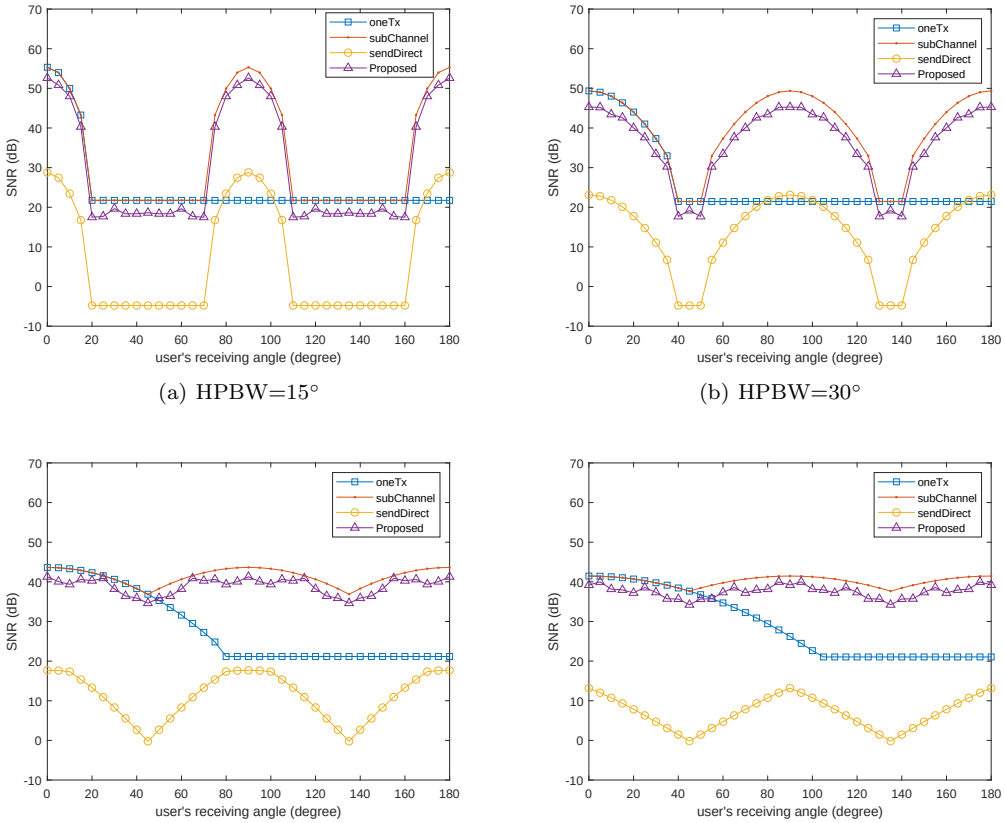

(a) HPBW=15° (b) HPBW=30°

(c) HPBW=60° (d) HPBW=80°

Fig. 3: SNR performance as a function of user's receiving angle under different HPBW angles

quality can be obtained in each reference scheme.

Fig. 4 shows the maximum supported video quality as a function of user's receiving angles. From the results, our proposed system can support 8K 360-degree video with 60 fps streaming irrespective of user's receiving angles. On the other hand, the other three schemes become lower video quality as the angle difference between the transmission antennas and user's device increases.

C. *Video Quality*

In this section, the PC streams the reconstructed 8K 360-degree video from the four transmission antennas to the user's HMD to discuss the received video quality in each reference scheme. Here, the ideal PSNR of the reconstructed at the PC quality is about 41.3 dB. All the schemes use BPSK as a modulation format. In this case, PSNR is zero even if one bit of the corresponding packet is erroneous.

Fig. 5 shows the received video quality of four schemes. Compared to the other schemes, even when the quality of the other schemes is significantly low, the proposed scheme yields better video quality. We believe that the proposed system can keep high received video quality by adopting some channel coding schemes.

D. *Discussion on Channel Capacity*

Fig. 6 shows the channel capacity as a function of transmission power at HPBW angle of 15 degree under the different user's receiving angles of 0 and 45 degrees. Compared to other schemes, our proposed system can provide a large channel capacity at the same distance and transmission power. It means the proposed system can reduce transmission power to meet the required capacity for uncompressed 360-degree video delivery.

5. Related Work

A. *Adaptive 360-Degree Video Streaming*

The adaptive 360-degree video streaming has been widely studied in recent years to efficiently deliver the videos over networks. The 360-degree videos are firstly projected into a 2D plane by different projection methods, such as equirectangular, cube-map, and pyramid projection. For the projected 360-degree videos, they use dynamic adaptive streaming over HTTP (DASH) for transmission over wired and wireless networks [16]. However, the delivery

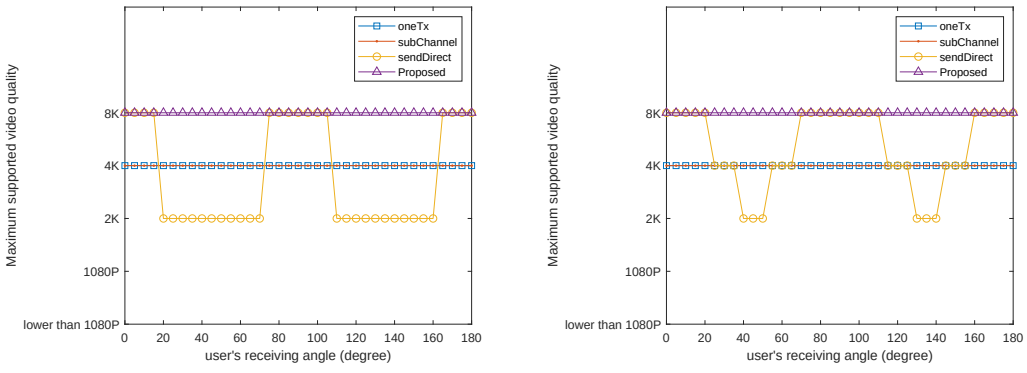

(a) HPBW=15° (b) HPBW=30°

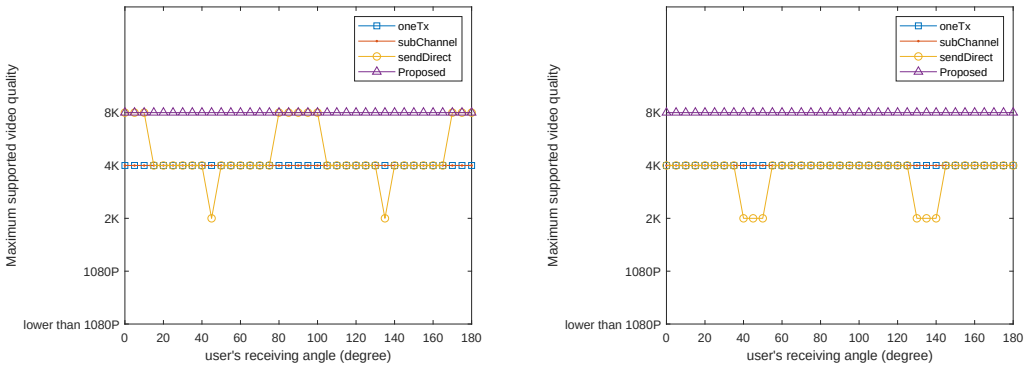

(c) HPBW=60° (d) HPBW=80°

Fig. 4: Maximum supported video as a function of user's receiving angle under different HPBW angles

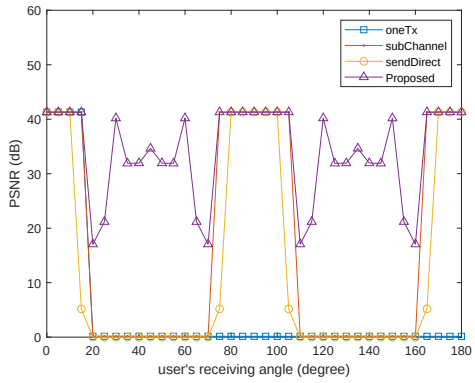

Fig. 5: PSNR performance as a function of user's receiving angles at HPBW angle of 15°

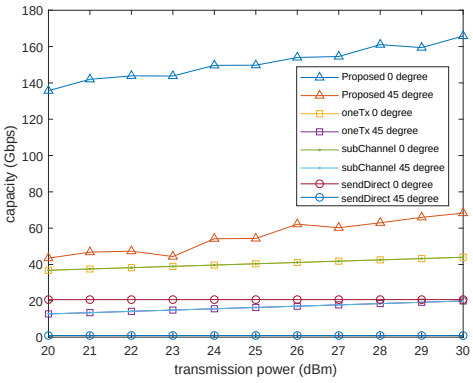

Fig. 6: Channel capacity as a function of transmission power at HPBW angle of 15° under the different user's receiving angles of 0 and 45 degrees

of full 360-degree may take a mass of bandwidth due to large traffic. Existing methods on 360-degree video delivery divide the projected video into multiple tiles and only a subset of tiles is transmitted to a user. Here, the existing adaptive 360-degree video streaming studies are mainly classified into two aspects: tiling-based and viewport-dependent streaming.

In tiling-based 360-degree video streaming, the tiles within the user's viewport are encoded into higher quality while the tiles out of the user's viewport are encoded into lower quality. To this end, [1] uses Scalable Video Coding (SVC) to encode the tiles into two layers to improve the quality of the viewport: base layer and enhancement layer. For quality optimization of tiling-based video streaming, [3] designs a tile-rate optimization and [8] considers storage costs for each tile optimization. In addition, other studies apply tile-based streaming to various

network conditions such as 5G wireless network [7] and software-defined network (SDN) [9] to discuss user's quality of experience (QoE).

In viewport-dependent streaming [2, 4–6, 10, 11], they only send the predicted user's future viewport for traffic reduction. For example, a head movement-aware streaming [10] and gaze-aware streaming with in-built eye tracker [4] have been proposed under the consideration of viewport prediction. Furthermore, by leveraging sensor- and content-related features, a fixation prediction network has proposed in [6,11] to predict the viewer fixation in the future. In addition, [2] observes the user's motion patterns when multiple users watch the same 360-degree video and proposes a multicast strategy for multi-user 360-degree video delivery based on motion prediction.

The proposed system is one of tiling-based 360-degree video streaming. Different from the existing studies, the proposed system sends the tiles of uncompressed 360-degree video from multiple 60 GHz mmWave antennas to greatly reduce the computing delay. In addition, the proposed system uses ZF-based precoding to avoid interference of the received signals.

B. Wireless Video Transmission Over MIMO System

The limited channel bandwidth and unpredictable propagation channel in wireless links make it difficult to provide immersive video contents such as multi-view video, free viewpoint video, and 360-degree video. To improve achievable channel bandwidth in the wireless links, the wireless MIMO systems emerge as one of the most prominent technologies.

The existing approach [17] uses SVC to generate bit streams with multiple layers so as to assign each layer of the bitstream to each antenna over adaptive channel selection MIMO (ACS-MIMO) system. In such a system, it periodically switches the transmission antenna for each bit stream. In [18,19], they design a resource allocation algorithm for multi-user MIMO (MU-MIMO) system. In [20], they study the optimal resource allocation using a nonlinear mixed integer programming framework for 3D content delivery with multi-view video coding over a MIMO system. In addition, a near-optimal power allocation scheme, targeting at QoE maximization, is also proposed for SVC-based video delivery over MIMO system [21].

Different from the existing studies, the proposed system uses multiple 60 GHz mmWave antennas for uncompressed 360-degree video delivery. By placing multiple antennas and assigning the predicted viewports to them, the proposed system enables the user to watch the desired viewport irrespective of direction.

C. mmWave-based Wireless Video Transmission

The compressed 360-degree video transmission through 2.4/5 GHz wireless networks may cause issues on delay-sensitive applications such as wireless VR due to insufficient network capacity and long computing delay. Recently, some studies utilize mmWave for wireless video streaming [22–26].

In [22], they proceed with a simple experiment on the 360-degree video transmission in indoor mmWave environments. Specifically, a sender sends Finite State Entropy (FSE) encoded 360-degree video and the receiver uses a high-end computer to decode high-quality 360-degree video in a short distance using mmWave. However, available bandwidth in mmWave communications suddenly decreases due to the blockage problem and headset movement in an indoor environment because mmWave is high directional. To address such issues, [24] proposes a novel system, called $MoVR$. The system supports multiple "mirrors" to add an alternative path to the headset. A reconfigurable 60 GHz reflect-arrays and a three-party beam-searching protocol are also designed to establish a robust connection when the links are blocked by barrier [23]. [25] leverages the pose information on mobile users to select the AP and [26] proposes a mmWave-based wireless access network called $UbiG$ which includes a fast probing based beam alignment algorithm and an infrastructure-side predictive ranking based fast access point switching algorithm.

In our research, we integrate mmWave, tiling, and MIMO for wireless 360-degree video delivery with low delay and high video quality. The advantage of mmWave is to provide sufficient bandwidth to transmit high-quality 360-degree video without compression. The tiling is to divide the uncompressed 360-degree video into multiple tiles for assigning each tile to each mmWave antenna. MIMO is used to reduce the burden of each antenna and to achieve stable 360-degree video delivery irrespective of HMD user's direction.

6. Conclusion

This paper proposes a novel system of wireless 360-degree video delivery. The proposed scheme deploys multiple 60

GHz antennas around the user to transmit uncompressed 360-degree video. In addition, each antenna enables the wireless HMD user to receive the corresponding viewport by using viewport prediction. Furthermore, ZF precoding reduces the interference between transmission antennas. Evaluations show that the proposed system can provide sufficient data rate for the delivery of the uncompressed 360-degree video with 8K resolution at 60 fps.

参考文献

[1] Nasrabadi, A. T., Mahzari, A., Beshay, J. D. and Prakash, R.: Adaptive 360-degree video streaming using scalable video coding, *Proceedings of the 25th ACM International Conference on Multimedia*, ACM, pp. 1689–1697 (2017).

[2] Bao, Y., Zhang, T., Pande, A., Wu, H. and Liu, X.: Motion-prediction-based multicast for 360-degree video transmissions, *14th Annual IEEE International Conference on Sensing, Communication, and Networking (SECON)*, IEEE, pp. 1–9 (2017).

[3] Rossi, S. and Toni, L.: Navigation-aware adaptive streaming strategies for omnidirectional video, *IEEE 19th International Workshop on Multimedia Signal Processing (MMSP)*, IEEE, pp. 1–6 (2017).

[4] Lungaro, P., Sjöberg, R., Valero, A. J. F., Mittal, A. and Tollmar, K.: Gaze-aware streaming solutions for the next generation of mobile VR experiences, *IEEE Transactions on Visualization and Computer Graphics*, Vol. 24, No. 4, pp. 1535–1544 (2018).

[5] Nguyen, D. V., Tran, H. T. and Thang, T. C.: Impact of delays on 360-degree video communications, *TRON Symposium (TRONSHOW)*, IEEE, pp. 1–6 (2017).

[6] Fan, C.-L., Lee, J., Lo, W.-C., Huang, C.-Y., Chen, K.-T. and Hsu, C.-H.: Fixation prediction for 360 video streaming in head-mounted virtual reality, *Proceedings of the 27th Workshop on Network and Operating Systems Support for Digital Audio and Video*, ACM, pp. 67–72 (2017).

[7] Graf, M., Timmerer, C. and Mueller, C.: Towards bandwidth efficient adaptive streaming of omnidirectional video over http: Design, implementation, and evaluation, *Proceedings of the 8th ACM on Multimedia Systems Conference*, ACM, pp. 261–271 (2017).

[8] Xiao, M., Zhou, C., Liu, Y. and Chen, S.: Optile: Toward optimal tiling in 360-degree video streaming, *Proceedings of the 25th ACM International Conference on Multimedia*, ACM, pp. 708–716 (2017).

[9] Zhao, S. and Medhi, D.: SDN-Assisted adaptive streaming framework for tile-based immersive content using MPEG-DASH, *IEEE Conference on Network Function Virtualization and Software Defined Networks (NFV-SDN)*, IEEE, pp. 1–6 (2017).

[10] Nguyen, D. V., Tran, H. T., Pham, A. T. and Thang, T. C.: A new adaptation approach for viewport-adaptive 360-degree video streaming, *IEEE International Symposium on Multimedia (ISM)*, IEEE, pp. 38–44 (2017).

[11] Borji, A., Cheng, M.-M., Hou, Q., Jiang, H. and Li, J.: Salient object detection: A survey, *arXiv preprint arXiv:1411.5878* (2014).

[12] Su-Khiong Yong, Samsung Advanced Institute of Technology, P.: IEEE 802.15.3c Channel Modeling Sub-committee Report, *IEEE 802.11ad-IEEE 802 LAN/MAN Standards Committee*, pp. 17–18 (2007).

[13] Alexander Maltsev, Vinko Erceg, E. P.: Channel Models for 60 GHz WLAN Systems, *IEEE 802.11ad-IEEE 802 LAN/MAN Standards Committee*, pp. 144–145 (2010).

[14] Wiesel, A., Eldar, Y. C. and Shamai, S.: Zero-Forcing Precoding and Generalized Inverses., *IEEE Trans. Signal Processing*, Vol. 56, No. 9, pp. 4409–4418 (2008).

[15] silex lite connect: SX-PCEAD 2017, `http://www.silex.jp/products/silex_lite_connect/sxpcead.html` (2017).

[16] Stockhammer, T.: Dynamic adaptive streaming over HTTP–: standards and design principles, *Proceedings of the second annual ACM conference on Multimedia systems*, ACM, pp. 133–144 (2011).

[17] Song, D. and Chen, C. W.: Scalable H. 264/AVC video transmission over MIMO wireless systems with adaptive channel selection based on partial channel information, *IEEE Transactions on Circuits and Systems for Video Technology*, Vol. 17, No. 9, pp. 1218–1226 (2007).

[18] Park, J., Chen, X. and Hwang, J.-N.: Optimal power allocation and rate adaptation for scalable video over multi-user MIMO, *2015 IEEE Global Communications Conference (GLOBECOM)*, IEEE, pp. 1–6 (2015).

[19] Tseng, S.-M. and Chen, Y.-F.: Average PSNR optimized cross layer user grouping and resource allocation for uplink MU-MIMO OFDMA video communications, *IEEE Access*, Vol. 6, pp. 50559–50571 (2018).

[20] Chen Z, Zhang X, X. Y.: MuVi: Multiview Video Aware Transmission Over MIMO Wireless Systems, *IEEE Transactions on Multimedia*, Vol. 19, No. 12, pp. 2788–2803 (2017).

[21] Chen X, Hwang J N, L. C. N.: A near optimal QoE-driven power allocation scheme for scalable video transmissions over MIMO systems, *IEEE Journal of selected topics in Signal Processing*, Vol. 9, No. 1, pp. 76–88 (2015).

[22] Le, T. T., Van Nguyen, D. and Ryu, E.-S.: Computing Offloading Over mmWave for Mobile VR: Make 360 Video Streaming Alive, *IEEE Access*, Vol. 6, pp. 66576–66589 (2018).

[23] Tan, X., Sun, Z., Koutsonikolas, D. and Jornet, J. M.: Enabling indoor mobile millimeter-wave networks based on smart reflect-arrays, *IEEE INFOCOM 2018-IEEE Conference on Computer Communications*, IEEE, pp. 270–278 (2018).

[24] Abari, O., Bharadia, D., Duffield, A. and Katabi, D.: Enabling High-Quality Untethered Virtual Reality, *14th USENIX Symposium on Networked Systems Design and Implementation (NSDI 17)*, Boston, MA, USENIX Association, pp. 531–544 (online), available from ⟨https://www.usenix.org/conference/nsdi17/technical-sessions/presentation/abari⟩ (2017).

[25] Wei, T. and Zhang, X.: Pose information assisted 60 ghz networks: Towards seamless coverage and mobility support, *Proceedings of the 23rd Annual International Conference on Mobile Computing and Networking*, ACM, pp. 42–55 (2017).

[26] Sur, S., Pefkianakis, I., Zhang, X. and Kim, K.-H.: Towards scalable and ubiquitous millimeter-wave wireless networks, *Proceedings of the 24th Annual International Conference on Mobile Computing and Networking*, ACM, pp. 257–271 (2018).